

Expansion of high-latitude deciduous forests driven by interactions between climate warming and fire

Zelalem A. Mekonnen ^{1*}, William J. Riley ¹, James T. Randerson², Robert F. Grant ³ and Brendan M. Rogers⁴

High-latitude regions have experienced rapid warming in recent decades, and this trend is projected to continue over the twenty-first century¹. Fire is also projected to increase with warming^{2,3}. We show here, consistent with changes during the Holocene⁴, that changes in twenty-first century climate and fire are likely to alter the composition of Alaskan boreal forests. We hypothesize that competition for nutrients after fire in early succession and for light in late succession in a warmer climate will cause shifts in plant functional type. Consistent with observations, our ecosystem model predicts evergreen conifers to be the current dominant tree type in Alaska. However, under future climate and fire, our analysis suggests the relative dominance of deciduous broadleaf trees nearly doubles, accounting for 58% of the Alaska ecosystem's net primary productivity by 2100, with commensurate declines in contributions from evergreen conifer trees and herbaceous plants. Post-fire deciduous broadleaf tree growth under a future climate is sustained from enhanced microbial nitrogen mineralization caused by warmer soils and deeper active layers, resulting in taller trees that compete more effectively for light. The expansion of deciduous broadleaf forests will affect the carbon cycle, surface energy fluxes and ecosystem function, thereby modifying important feedbacks with the climate system.

High-latitude warming during the twenty-first century increases the potential for changes in vegetation growth, decomposition of soil organic matter and net ecosystem carbon balance⁵, which in turn may contribute to feedbacks with the climate system^{1,6}. Potential transitions between deciduous and evergreen vegetation^{7–9} are of considerable interest because they are uncertain in current projections and fundamentally change ecosystem carbon dynamics, energy budgets, regional water balance, fire regimes, wildlife habitat and ecosystem services. Palaeoecological studies of the Holocene suggest that Alaskan forests have undergone shifts in dominant tree species driven by changes in climate and disturbance regimes (primarily fire)⁴. Aspen (*Populus tremuloides*), a deciduous broadleaf tree, was dominant in Alaskan boreal forests in the early Holocene, which was warmer and drier compared to the present. During the late Holocene (which was slightly cooler with similar precipitation compared to present^{4,10}), the evergreen conifer, black spruce (*Picea mariana*), became dominant, a stable state which has persisted to the present¹¹.

Several high-latitude experimental manipulations that mimic future warming have shown overall increases in ecosystem

productivity^{12,13}. However, interactions between warming and fire and their effects on vegetation dynamics have not been systematically explored in these warming experiments, leaving uncertain an important aspect of long-term vegetation responses to climate change.

High-latitude fire interacts with climate through effects on vegetation structure and function^{8,14}, the surface energy budget¹⁵, soil organic carbon stocks¹⁶, seedbed quality⁷ and nutrient availability¹⁷, all of which are interconnected. The loss of the insulating surface's organic matter¹⁶ and increases in soil heat fluxes¹⁵ after fire deepen the active layer¹⁸, leading to more rapid mineralization and increases in short-term nutrient availability^{19,20} for plant uptake. These early successional transient changes in nutrient cycling create a new environment for plants to compete for nutrients.

We applied a well-tested mechanistic model, ecosys²¹, and examined how plant functional types (evergreens, graminoids, deciduous and non-vascular (moss and lichen) plants) across the boreal forests of Alaska respond to projected twenty-first century changes in climate and fire regime. A number of studies have described potential future shifts in high-latitude vegetation types, including changes in boreal tree composition^{7,8,22,23} and the expansion of tree cover in the transition zone between the boreal forest and the Arctic tundra²⁴. Building on that work, our study highlights the importance of mechanistically representing differences in plant functional traits (Methods) and their emergent effects on current and possible twenty-first century trajectories of tree compositions in Alaska. Changes in plant functional types were modelled prognostically from competitive processes regulating nutrient and water uptake, radiation interception, and internal carbon and nutrient cycling and retention.

The model was rigorously and successfully tested against observations from eddy-covariance flux towers in many high-latitude sites across multiple years and against large-scale remote-sensing vegetation observations (Supplementary I Methods). We initialized the model with a temporally static dataset of soil attributes and then forced the model in transient simulations with temporally dynamic nitrogen deposition fluxes, atmospheric CO₂ concentrations, fire and climate from 1800 to 2100 at a 0.25° × 0.25° spatial resolution (Methods; Supplementary I Table 1). The historical climate data were derived from the North American Regional Reanalysis (NARR)²⁵. The twenty-first century climate forcing was from the Representative Concentration Pathway 8.5 (RCP8.5), downscaled and averaged from 15 Coupled Model Intercomparison Project phase 5 (CMIP5) model projections²⁶ (Supplementary I Tables 1 and 2). Past fire events were modelled statistically using the map

¹Climate and Ecosystem Sciences Division, Lawrence Berkeley National Laboratory, Berkeley, CA, USA. ²Department of Earth System Science, University of California, Irvine, CA, USA. ³Department of Renewable Resources, University of Alberta, Edmonton, Canada. ⁴Woods Hole Research Center, Falmouth, MA, USA. *e-mail: zmekonnen@lbl.gov

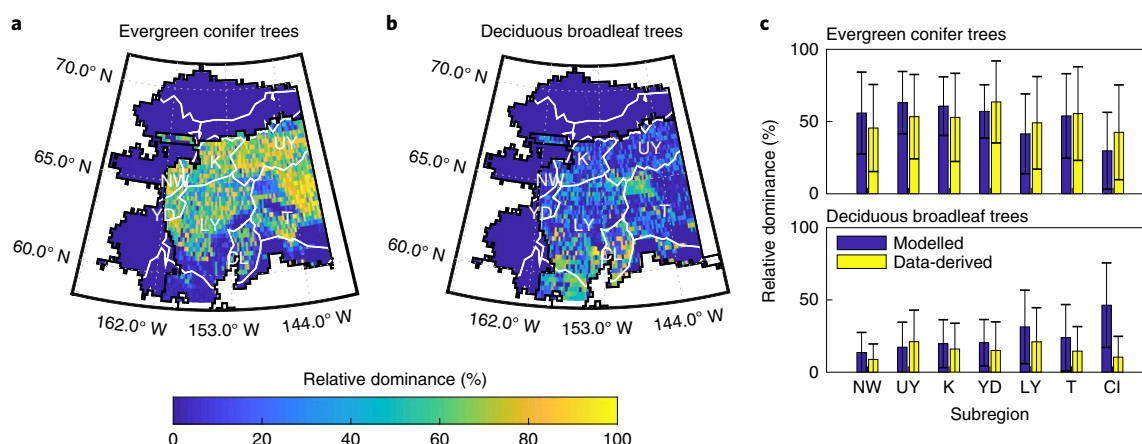


Fig. 1 | The model broadly reproduced the current tree composition of the Alaskan boreal forest. a,b, The LAI-based relative dominance for modelled evergreen conifer trees (42%) (**a**) and deciduous broadleaf trees (24%) (**b**) compared well with land cover derived from LANDFIRE–FCCS maps¹⁴ aggregated to $0.25^{\circ} \times 0.25^{\circ}$ spatial resolution across the Alaskan boreal forest (42% and 12%, respectively). **c**, The modelled relative dominance also compared very well with FCCS data-derived estimates for seven subregions within the boreal forest: NW, Northwest; UY, Upper Yukon; K, Koyukuk; YD, Yukon Delta; LY, Lower Yukon; T, Tanana; CI, Cook Inlet. The error bars represent standard deviations computed from grid cell values within the spatial domain of each subregion. The spatial correlation of the boreal forest's relative dominance between modelled LAI and LANDFIRE–FCCS land cover using a geographically weighted regression was $R^2 = 0.77$ for evergreen conifer trees and $R^2 = 0.65$ for deciduous broadleaf trees.

of mean fire return interval from the United States' Landscape Fire and Resource Management Planning Tools (LANDFIRE) product²⁷, which estimates the average time between fire events (Methods; Supplementary I Fig. 1) and which we take as the contemporary baseline. The projected increases in burned area over the twenty-first century were applied to this baseline (a 71% increase by 2100) and were derived from projected changes in lightning ignition³. We conducted seven sensitivity simulations to test the effects on boreal forest vegetation dynamics of area burned, fire severity, post-fire seedling regeneration and changes in precipitation (Methods; Supplementary I Table 3).

To assess the model's performance within our study domain of Alaska, we compared the modelled leaf area index (LAI) against land cover derived from LANDFIRE's Fuel Characteristic Classification System (FCCS) maps¹⁴ aggregated to a $0.25^{\circ} \times 0.25^{\circ}$ resolution for consistency with the model simulations (Fig. 1). Under the current climate, evergreen conifers were modelled to be the dominant trees of mature stands across boreal Alaska (Fig. 1). The model estimates of relative dominance (defined as [plant functional type LAI/ecosystem LAI] $\times 100$) in the boreal forest were 42% for evergreen conifers and 24% for deciduous broadleaf trees, which were broadly consistent with the LANDFIRE–FCCS estimates of 42% and 12%, respectively (Fig. 1). We also compared the relative dominance of evergreen conifers and deciduous broadleaf trees for seven subregions of the boreal forest and found good agreement with model predictions (Fig. 1c). The relative dominance of the modelled evergreen conifer trees was also consistent with another study reporting an evergreen conifer tree proportion of 44% from a set of intensively studied field sites in interior Alaska¹¹.

We also evaluated the modelled gross primary productivity (GPP) and biomass across Alaskan boreal forests using GPP upscaled from a network of eddy-covariance observations ($R^2 = 0.67$) and data-derived biomass estimates ($R^2 = 0.59$) (Supplementary I Fig. 2). The model also compared well against fine-scale (hourly) surface energy fluxes (net radiation, sensible heat and latent heat; $R^2 = 0.52$ – 0.79) and hourly CO_2 fluxes ($R^2 = 0.59$ – 0.73) measured at eddy-covariance flux towers in 2003 at three different stands in a fire chronosequence at Delta Junction (Supplementary I Figs. 3 and 4). Finally, the model reproduced many aspects of observed post-fire successional change in vegetation cover²⁸ (Fig. 2a–c; Supplementary I Fig. 5).

We found that plant functional type competition for nutrients and light were key controls on post-fire successional trajectories (Fig. 2 and Supplementary I Fig. 6). Under both the twentieth and twenty-first century climates, the higher net absorbed energy by the exposed soil after vegetation and surface litter removal increased the post-fire 0–30-cm soil temperature for several years by about 4.5°C , albeit from different starting temperatures (Fig. 2c,f). The warmer soil increased nitrogen mineralization from rapid decomposition of fine non-woody surface residue, which resulted in a short-term increase in post-fire nitrogen availability. This initial pulse of mineralized nitrogen after fire (the assart effect²⁰) caused rapid nitrogen uptake mainly by herbaceous plants (non-vascular and graminoid; Fig. 2b,e). Short-term nitrogen uptake was also greater for deciduous broadleaf trees than for evergreen conifer trees.

We found that the increase in a plant's non-structural nitrogen content from rapid nitrogen mineralization and plant uptake after fire resulted in greater CO_2 fixation primarily by low-lying herbaceous plants and deciduous broadleaf trees (Fig. 2a,d), thus allowing these plant functional types to attain higher levels of net primary productivity (NPP) compared to evergreen conifer trees for the first 5 years after fire. Between 5 and 20 years after fire, the decomposition of the coarse woody litter with higher modelled carbon-to-nitrogen ratios resulted in (1) immobilization, and therefore a decline in soil mineral nitrogen; and (2) a gradual levelling of plant nitrogen uptake (Fig. 2b,e), and therefore carbon gains by herbaceous and deciduous broadleaf plant functional types (Fig. 2a,d). The more conservative strategy of evergreen conifer trees allows for slower but continuous increases in carbon uptake under nitrogen-limited conditions compared to deciduous broadleaf trees. This difference was modelled through differences in traits for carbon and nutrient acquisition and retention: slower uptake and greater retention in evergreen conifer trees versus rapid uptake and loss (by means of litterfall) of nutrients in deciduous broadleaf trees²⁹. Compared to deciduous broadleaf trees, these modelled traits caused evergreen conifer trees to fix more carbon per leaf nitrogen invested, resulting in a higher nitrogen-use efficiency (for example, 330 versus 194 gC gN^{-1} , respectively, in 2010) (Supplementary I Fig. 7). This inherent trait of evergreen conifer trees provides them with a greater ability to compete in nitrogen-limited conditions³⁰.

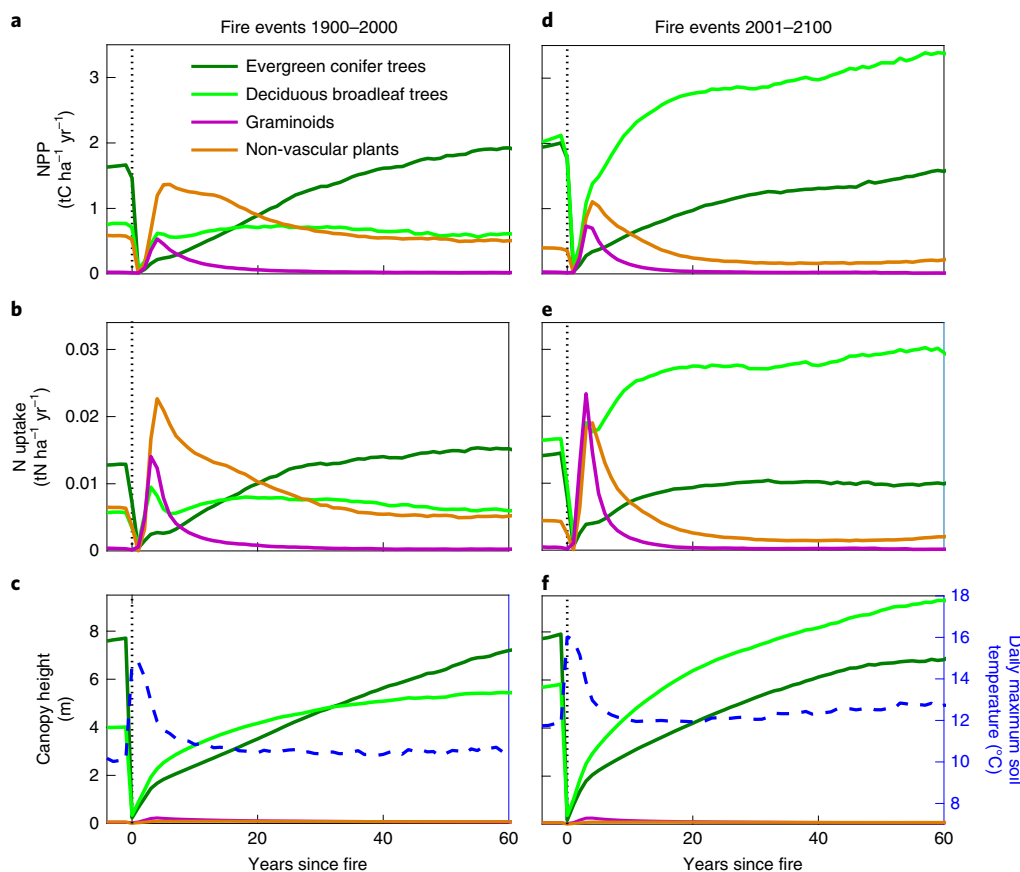


Fig. 2 | Modelled post-fire trajectories under the twentieth century climate differed from those under the twenty-first century climate. **a–f**, Modelled spatially averaged boreal forest pre- and post-fire: annual NPP (**a,d**), annual cumulative nitrogen uptake (**b,e**) and mid-August canopy height of Alaska coexisting plant function types (evergreen conifer trees, deciduous broadleaf trees, graminoids and non-vascular (moss + lichen) plants) and mid-August daily maximum 0–30 cm soil temperature (**c,f**) during fire events under twentieth century (**a,b,c**) and twenty-first century (**d,e,f**) climates. The vertical dotted grey lines indicate time of fire (that is, year 0). The NPP and nitrogen uptake values during the fire year were accumulated from days before the prescribed fire events (mid-August).

In later successional stages (>20 years) under twentieth century climate, we found that microbial decomposition of coarse woody litter lowered carbon-to-nitrogen ratios, resulting in a net mineralization and a continued increase in nitrogen uptake (Fig. 2b) and carbon gains (Fig. 2a) by evergreen conifer trees. With slower but continuous carbon gains, the evergreen conifer trees were modelled to have the tallest canopies after about 30 years, thus outcompeting the herbaceous plants and deciduous broadleaf trees for light (Fig. 2a,c). Under the twentieth century climate and fire regime, the deciduous broadleaf trees and herbaceous plants were modelled to contribute about 29% and 26% of the Alaskan boreal forest's NPP, respectively (Supplementary I Table 4).

Over the twenty-first century, nitrogen mineralization from fire-induced soil warming was enhanced through increases in surface air temperature (Supplementary I Table 2). An increase in heat advection and soil thermal conductivity from projected increases in precipitation also deepened the active layer and increased microbial decomposition. The average soil temperatures from 5 to 20 years after fire under the twenty-first century climate were about 1.5°C warmer than under the twentieth century climate (Fig. 2c,f). The warmer soils in the future resulted in greater amounts of available mineralized nitrogen, which enabled post-fire deciduous broadleaf trees to sustain continued rapid nitrogen uptake and CO₂ fixation (Fig. 2d,e). The increased nitrogen uptake was driven by greater leaf nutrient demand and less leaf clumping in deciduous broadleaf trees, which led to increased nutrient uptake capacity, leaf nutrient

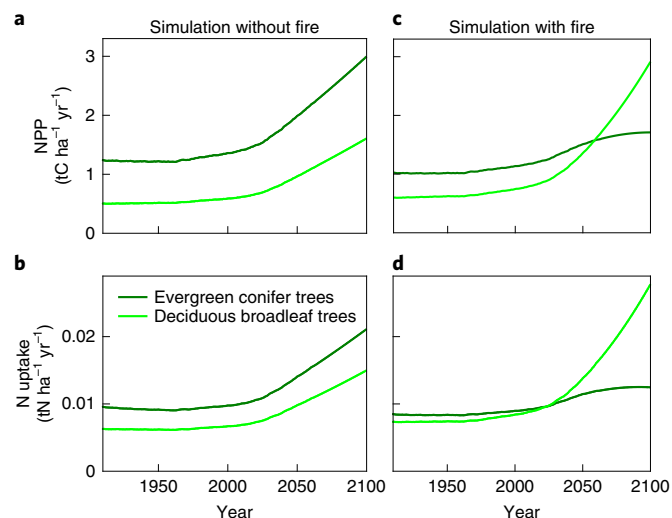


Fig. 3 | Deciduous broadleaf trees become dominant around 2058 because of interactions between increased soil temperatures, mineralization and fire. **a–d**, The modelled twentieth and twenty-first century spatially averaged Alaskan annual net primary productivity (NPP) (**a,d**) and cumulative nitrogen uptake (**b,d**). The left-hand column (**a,b**) shows the simulations without fire and the right-hand column (**c,d**) shows the simulations with fire (the scenario with a 71% increase in burned area by 2100).

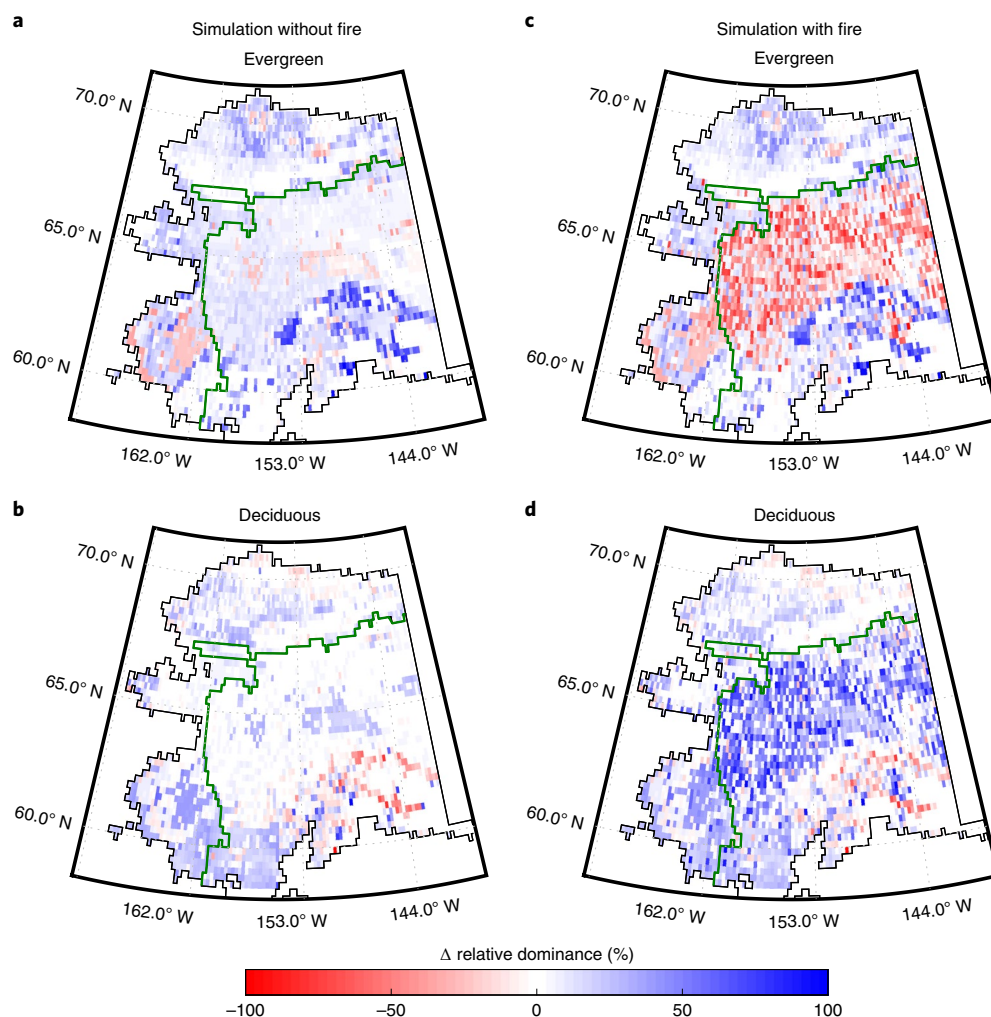


Fig. 4 | Deciduous broadleaf trees increase and evergreen conifer trees decrease in interior Alaska by 2100 because of warming and fire in the boreal forest. a–d, The modelled changes in the relative dominance of plant functional types from current to 2100 for evergreen conifers (**a,c**) and deciduous broadleaf trees (**b,d**). The left-hand column (**a,b**) shows the simulations without fire and the right-hand column (**c,d**) shows the simulations with fire (a 71% increase in burned area by 2100). The solid green line represents the boundary between the Arctic tundra (north and west) and boreal forest (south and east) ecosystems. The relative dominance of both deciduous and evergreen shrubs was shown to increase in much of the Arctic tundra, particularly on the North Slope of the Brooks Range, which is consistent with field experiments and observations indicating that climate warming will increase shrub cover in Arctic tundra⁴⁹.

concentrations and CO₂ fixation. Modelled leaf nutrient content influenced maximum carboxylation rates and electron transport. The modelled smaller leaf mass per area and less leaf clumping in deciduous broadleaf trees resulted in greater light interception for a given leaf carbon investment³¹. Rapid water uptake from modelled lower axial resistivity in deciduous broadleaf trees versus evergreen conifer trees also led to faster growth.

Our model predicted that by 2100, the NPP-based relative dominance of Alaskan deciduous broadleaf trees nearly doubled (Supplementary I Table 4), the dominance of evergreen conifer trees declined by about 25% and the dominance of non-woody herbaceous plants declined by about 66%. During the twenty-first century, the NPP of evergreen conifer trees did not recover to pre-fire levels even 60 years after fire (Fig. 2d) because of shading by deciduous broadleaf trees with rapid and sustained post-fire growth and thus greater canopy height (Fig. 2f) and LAI (Supplementary I Fig. 8). These simulation results suggest that competition for light is likely to be more important than competition for nutrients in determining tree dominance in later successional stages in a warmer future climate.

The model simulations forced with warming under a twenty-first century climate in the absence of fire resulted in evergreen conifers remaining the dominant Alaskan tree type (Fig. 3a). However, when fire was included in the simulations, deciduous broadleaf trees became dominant by 2058. These results indicate that (1) climate change in the absence of fire or (2) fire in the absence of climate change each were insufficient to cause a shift in the relative dominance of evergreen conifers to deciduous broadleaf trees despite a brief deciduous and herbaceous phase immediately after fire (Fig. 2a).

The ecosystem's NPP (Fig. 3a,c; Supplementary I Fig. 9) and LAI (Supplementary I Fig. 8) were modelled to increase in the twenty-first century mainly due to increased rates of CO₂ fixation and indirectly through warming-induced changes in nutrient cycling. Changes in the relative dominance of each plant functional type in response to climate and fire in the twenty-first century were spatially heterogeneous (Fig. 4). The greatest shift in relative dominance of evergreen conifers to deciduous broadleaf trees occurred in the interior of Alaska and in the Yukon delta, where fire events were most frequent (Fig. 4c,d; Supplementary I Fig. 1a). The relative

dominance of deciduous broadleaf trees was projected to be more than 50% in most of these regions by 2100 (Fig. 4d), with concurrent declines in evergreen conifer trees (Fig. 4a).

Overall, our results suggest that fire will serve as an agent together with twenty-first century warming to expand the distribution of deciduous broadleaf trees, making them dominant in northern boreal forest ecosystems (Fig. 3c). This projection is consistent with Holocene palaeoecological evidence in Alaskan forests^{4,10}, which indicates that deciduous broadleaf trees were dominant when the climate was warmer and evergreen conifer trees were dominant when the climate was cooler. Despite the differences in the causes of warming between the Holocene and the twenty-first century (that is, natural versus anthropogenic), the contrasting changes in climate and the resulting species composition are similar, supporting our model predictions of expected shifts in plant functional type.

To assess the sensitivity of our model projections to well-known drivers of vegetation dynamics in boreal forest ecosystems, we performed several Alaska-wide twenty-first century simulations in which we manipulated burned area, fire severity, post-fire seedling regeneration and precipitation. First, we found that the timing of the deciduous broadleaf tree dominance depended on the projected increases in burned area, advancing by about 9 years for a scenario with a 150% increase in burned area compared to our baseline scenario, which had a 71% increase in burned area (Supplementary I Fig. 10). Second, if fire severity were to increase in the future², favouring recruitment of deciduous broadleaf trees^{7,22}, our sensitivity analysis suggested an advance of deciduous broadleaf tree dominance by about 5 years (Supplementary I Fig. 11). Third, our precipitation trends sensitivity analyses suggested that if precipitation increases faster than the CMIP5 mean, the transition to deciduous dominance would advance by about 3 years (Supplementary I Fig. 12). Fourth, increases in fire severity² alone had a small positive effect on the transition from dominance by evergreen conifers to dominance by deciduous broadleaf trees. Other factors that may affect vegetation shifts over the twenty-first century, which we were unable to consider here, include three-dimensional changes in landscape-scale hydrological dynamics, heterogeneity in soil processes at a finer scale than the grid cells, limits to fire spread from deciduous broadleaf tree impacts on fuel moisture, topography, and disturbances by pests and pathogens.

The expansion of the boreal deciduous broadleaf forest in a warmer climate may result in several ecological and climatic feedbacks that affect the carbon cycle of northern ecosystems. Increases in deciduous broadleaf trees would increase the surface litter input and lower the litter's lignin content and carbon-to-nitrogen ratios, thus creating a positive feedback to more rapid microbial decomposition and nutrient cycling, which in turn lowers the overall ecosystem carbon residence times (Supplementary I Fig. 13). Increases in the proportion of deciduous broadleaf trees would also likely change seasonal phenology, with rapid increases in LAI associated with leaf onset in spring and subsequent declines in fall associated with leaf senescence (Supplementary I Fig. 14). From a climate perspective, a shift to deciduous tree dominance would increase transpiration and thus the influence of water vapour on longwave radiative forcing during summer³². Simultaneously, a higher surface albedo would have a cooling effect during fall, winter and spring, when more snow is exposed¹⁴. Declines in herbaceous plant productivity may affect the amount and distribution of summer forage³³ and thus change the habitat for moose and other animals. Deciduous broadleaf trees are less flammable than evergreen conifer trees³⁴, thus the shift in relative dominance may suppress fire¹⁴ and partly offset the increase in fire expected under a warmer climate. We conclude that these complex fire–vegetation–climate interactions have the potential to strongly affect high-latitude vegetation and carbon dynamics and that land models must therefore account for them to accurately capture long-term land surface–climate interactions.

Methods

The model, *ecosys*, includes multiple canopy and soil layers and fully coupled data on carbon, energy, water and nutrient cycles at an hourly time-step resolution. Surface energy and water exchanges drive soil heat and water transfers to determine soil temperatures and soil-water content in multiple soil layers. These transfers drive soil freezing and thawing, and therefore active layer depth, through the general heat flux equation. Carbon uptake is controlled by a plant's water status, which is calculated from convergence solutions that equilibrate the total root water uptake with transpiration. Atmospheric warming increases surface heat advection, soil heat transfers, and hence active layer depth. Canopy temperatures affect CO₂ fixation rates due to effects on carboxylation and oxygenation rates modelled with Arrhenius functions for light and dark reactions. Soil temperatures affect heterotrophic respiration through the same Arrhenius function as for dark reactions.

Carbon uptake is also affected by a plant's nitrogen uptake. The model represents fully coupled transformations of soil carbon, nitrogen and phosphorus through microbially driven processes. Soil warming enhances carbon uptake by hastening microbial mineralization and root nitrogen uptake. Carbon uptake is affected by phenology; leafout and leafoff (deciduous plants) or dehardening and hardening (evergreen plants) are determined by accumulated exposure to temperatures above the set values while the day length is increasing or below the set values while the day length is decreasing. Senescence is driven by excess maintenance respiration and by phenology in deciduous plant functional types. A detailed description of inputs, parameters and algorithms used in *ecosys* is found in Supplementary Information II.

Plant functional type dynamics. The model represents basic plant functional type-specific traits (for example, specific leaf area (leaf area-to-mass ratio), leaf optical properties, leaf clumping, leaf turnover, foliar nutrient content, foliar nutrient retention and root hydraulic conductivity) that are known to differ among plants³⁵. These traits drive modelled differences in carbon and nutrient investment and retention strategies in leaves, stems and roots.

Deciduous broadleaf trees are modelled to have greater specific leaf area and less leaf clumping (self-shading) and thus greater light interception as compared to evergreen conifer trees. Deciduous broadleaf trees are modelled to have full annual leaf turnover, whereas evergreen conifer trees retain their leaves. Nutrient conservation during litterfall is driven by carbon, nitrogen and phosphorus recycling coefficients, which increase with non-structural carbon-to-nitrogen ratios³⁶. A higher remobilization of resources is modelled to occur in evergreen conifer trees, enabling them to compete more effectively than deciduous broadleaf trees in nutrient-limited environments^{35,37}.

Broadleaf deciduous trees are modelled to have higher potential leaf nitrogen and phosphorus concentrations under non-limiting nitrogen and phosphorus conditions than evergreen conifer trees. Under actual nutrient-limiting conditions, modelled leaf nutrient concentrations are dynamic and often below these potential values. Actual leaf nutrient concentration affects modelled maximum carboxylation rates and electron transport. Greater nutrient demand and investment in nutrient uptake capacity drives higher nutrient uptake and CO₂ fixation in deciduous broadleaf when compared with evergreen conifer trees.

Lower axial resistivity is modelled in deciduous broadleaf trees, allowing faster water uptake and thus faster nitrogen uptake and growth (a less conservative and faster growing strategy)^{35,36}. A higher axial resistance in evergreen conifer trees slows water uptake and reduces stomatal conductance, carbon fixation and growth.

These differences in plant traits result in emergent variations in phenology, irradiance, CO₂ fixation rate and water uptake among plant functional types and thus their ability to compete. These processes drive vertical profiles of leaf area and root length that determine competition for radiation, water and nutrients within each canopy and rooted soil layer, depending on leaf area and root length. The vertical profiles are generated from allocations of a plant's non-structural carbon, nitrogen and phosphorus to each organ of each plant functional type³⁵. The interception of incoming direct and diffuse radiation and backscattering is resolved across each canopy layer. Each plant functional type competes for nutrient and water uptake, depending on root length and density and driven by the allocation of non-structural carbon, nitrogen and phosphorus.

Simulation design. We initialized the seed densities and total seed carbon for coexisting plant functional types (deciduous, evergreen, sedge, moss, lichen) across the simulation spatial domain. The model was initialized with soil attributes obtained from the Unified North America Soil Map³⁸ (clay and sand fraction, pH, cation exchange capacity, bulk density) and the Northern Circumpolar Soil Carbon Database³⁹ (soil organic carbon) gridded to a 0.25° × 0.25° spatial resolution across vertical soil profiles (Supplementary I Table 1). The model was forced with the temporally dynamic climate, atmospheric CO₂ concentrations, fire and nitrogen deposition from 1800 to 2100. The nitrogen deposition data were derived from global atmospheric nitrogen deposition maps^{40,23}. Climate forcing (surface air temperature, precipitation, incoming shortwave radiation, relative humidity and wind speed) from 1979 to 1988 was taken from the NARR and cycled through 1800 to 1978. The earlier 10 years of NARR were selected to reduce the effects of amplified warming events during the later years, on model spin-up. The full NARR

time series was used to force the model from 1979 to 2010. The coarser temporal resolution of time-varying model inputs were interpolated linearly to 1 h for use in ecosystems. Uncertainties in modelled outputs associated with coarser resolution gridded model inputs⁴¹ should be noted and may not be avoided given the available datasets. The changes in climate over the twenty-first century were derived from the RCP8.5 scenario ensemble projections, which were downscaled and averaged across 15 CMIP5 models (Supplementary I Table 2). We chose the RCP8.5 climate scenario because the current trend of global carbon emissions from 2006 to 2017 was increasing at a rate that was broadly consistent with this high emissions scenario.

Disturbance caused by stand-replacing fire was prescribed as an external forcing in the model. The impacts of twentieth century and twenty-first century climate and fire on the Alaskan plant functional type dynamics were examined in model sensitivity simulations (model simulations forced with twentieth and twenty-first century climates in the absence of fire versus simulations under presumed past and projected future fire activity). These sensitivity runs were used to partition the effects of (1) a warmer climate in the twenty-first century compared with the climate of the twentieth century and (2) the combined effects of fire and a future warmer climate compared with the past climate on plant functional type dynamics of Alaska.

Past fire frequency was derived from the Mean Fire Return Interval (MFRI) dataset of the LANDFIRE product²⁷, which estimates the average time between presumed past fire events (Supplementary I Fig. 1). The MFRI dataset was developed by the US Forest Service using vegetation, fuel characteristics and historical disturbance information in each 30-m grid cell. A temporal distribution of individual fire events during 1800 to 2010 was prescribed in ecosystems on the basis of stand-age-dependent fire-event-return intervals generated from a normal distribution of the base MFRI for each grid cell. The probability of fire occurrence in a grid cell was set to be dependent on the stand age: fire probability was low immediately following a fire event within a grid cell and then linearly increased with stand age. This approach allowed ecosystems to mimic observations that there was a lower probability of a subsequent fire within areas that recently burned and implicitly limited the chance of burning in the early successional stages that tended to have greater dominance by herbaceous plants and deciduous broadleaf trees. The projected increases in burned area over the twenty-first century were applied to the base MFRI using an estimated rate of increase (71% increase in burned area by 2100 (ref. 3)) obtained from relations between the changes in climate variables under the RCP8.5 climate change scenario with the changes in lightning ignition taken from Veraverbeke et al.³. All fire events were set as 'stand-replacing' with prescribed fractions of combusted below- and above-ground biomass, soil organic carbon, nitrogen and phosphorus. In addition to direct losses of nutrients from combustion, the model also simulates losses from leaching. We prescribed a depth of burn to 15.1 cm on the basis of the mean depth of burn data^{42–44} from 235 burned sites across Alaska.

We also conducted seven sensitivity simulations to test the effects of changes in area burned, fire severity, post-fire seedling regeneration and precipitation on the vegetation dynamics of the boreal forest (Supplementary I, Table 3). The projected increases in burned area are uncertain^{2,45}; to address this uncertainty, we conducted two more scenarios of projected increases in burned area over the twenty-first century (0% change in burned area and 150% (average prediction of fire models^{16–48}) increase in burned area by 2100). The sensitivity to changes in fire severity and depth of burn during the twenty-first century were tested by linearly increasing the depth of burn from 15.1 cm in 2010 to 26.5 cm (the 95th percentile of data from the 235 burned sites) in 2100. To test the impact of fire on vegetation dynamics through its effect on post-fire seedbed quality (and thus the germination of the seedlings), we conducted a separate simulation by filtering the post-fire tree seedlings to ~75% deciduous broadleaf trees versus ~25% evergreen conifer trees on the basis of data from 90 burned sites in Alaska taken from Johnstone et al.⁷. To test the sensitivity of modelled vegetation dynamics to changes in projected precipitation trends, we conducted two separate simulations driven by a lower and a higher twenty-first century precipitation trend compared to the mean of the 15 CMIP5 models under the RCP8.5 scenario.

Reporting Summary. Further information on research design is available in the Nature Research Reporting Summary linked to this article.

Data availability

Data products in this study are archived at <http://ngee-arctic.ornl.gov>. Additional data that support the findings of this study can be found from the corresponding author upon request.

Received: 29 November 2018; Accepted: 16 July 2019;

Published online: 26 August 2019

References

- IPCC *Climate Change 2013: The Physical Science Basis* (eds Stocker, T. F. et al.) (Cambridge Univ. Press, 2013).
- Flannigan, M., Stocks, B., Turetsky, M. & Wotton, M. Impacts of climate change on fire activity and fire management in the circumboreal forest. *Glob. Change Biol.* **15**, 549–560 (2009).
- Veraverbeke, S. et al. Lightning as a major driver of recent large fire years in North American boreal forests. *Nat. Clim. Change* **7**, 529 (2017).
- Lloyd, A. H. et al. in *Alaska's Changing Boreal Forest* (eds Chapin, F. S. III et al.) 62–78 (Oxford Univ. Press, 2006).
- Qian, H., Joseph, R. & Zeng, N. Enhanced terrestrial carbon uptake in the northern high latitudes in the 21st century from the coupled carbon cycle climate model intercomparison project model projections. *Glob. Change Biol.* **16**, 641–656 (2010).
- Euskirchen, E. S., McGuire, A. D., Chapin, F. S. III, Yi, S. & Thompson, C. C. Changes in vegetation in northern Alaska under scenarios of climate change, 2003–2100: implications for climate feedbacks. *Ecol. Appl.* **19**, 1022–1043 (2009).
- Johnstone, J. F., Hollingsworth, T. N., Chapin, F. S. & Mack, M. C. Changes in fire regime break the legacy lock on successional trajectories in Alaskan boreal forest. *Glob. Change Biol.* **16**, 1281–1295 (2010).
- Mann, D. H., Rupp, T. S., Olson, M. A. & Duffy, P. A. Is Alaska's boreal forest now crossing a major ecological threshold? *Arct. Antarct. Alp. Res.* **44**, 319–331 (2012).
- Johnstone, J. F. et al. Fire, climate change, and forest resilience in interior Alaska. *Can. J. For. Res.* **40**, 1302–1312 (2010).
- Edwards, M. E., Brubaker, L. B., Lozhkin, A. V. & Anderson, P. M. Structurally novel biomes: a response to past warming in Beringia. *Ecology* **86**, 1696–1703 (2005).
- Van Cleve, K. et al. Taiga ecosystems in interior Alaska. *Bioscience* **33**, 39–44 (1983).
- Strömgen, M. & Linder, S. Effects of nutrition and soil warming on stemwood production in a boreal Norway spruce stand. *Glob. Change Biol.* **8**, 1194–1204 (2002).
- McPartland, M. Y. et al. The response of boreal peatland community composition and NDVI to hydrologic change, warming, and elevated carbon dioxide. *Glob. Change Biol.* **25**, 93–107 (2019).
- Rogers, B. M., Soja, A. J., Goulden, M. L. & Randerson, J. T. Influence of tree species on continental differences in boreal fires and climate feedbacks. *Nat. Geosci.* **8**, 228–234 (2015).
- Liu, H., Randerson, J. T., Lindfors, J. & Chapin, F. S. III Changes in the surface energy budget after fire in boreal ecosystems of interior Alaska: An annual perspective. *J. Geophys. Res. Atmos.* **110**, D13 (2005).
- Mack, M. C. et al. Carbon loss from an unprecedented Arctic tundra wildfire. *Nature* **475**, 489–492 (2011).
- Neff, J., Harden, J. & Gleixner, G. Fire effects on soil organic matter content, composition, and nutrients in boreal interior Alaska. *Can. J. For. Res.* **35**, 2178–2187 (2005).
- Genet, H. et al. Modeling the effects of fire severity and climate warming on active layer thickness and soil carbon storage of black spruce forests across the landscape in interior Alaska. *Environ. Res. Lett.* **8**, 045016 (2013).
- Driscoll, K., Arocena, J. & Massicotte, H. Post-fire soil nitrogen content and vegetation composition in sub-boreal spruce forests of British Columbia's central interior, Canada. *For. Ecol. Manag.* **121**, 227–237 (1999).
- Kimmins, J. P. *Forest Ecology: A Foundation for Sustainable Forest Management and Environmental Ethics in Forestry* (Prentice Hall, 2004).
- Grant, R. F. et al. Interannual variation in net ecosystem productivity of Canadian forests as affected by regional weather patterns—A Fluxnet-Canada synthesis. *Agric. For. Meteorol.* **149**, 2022–2039 (2009).
- Johnstone, J. F., Rupp, T. S., Olson, M. & Verbyla, D. Modeling impacts of fire severity on successional trajectories and future fire behavior in Alaskan boreal forests. *Landsc. Ecol.* **26**, 487–500 (2011).
- Chaste, E., Girardin, M. P., Kaplan, J. O., Bergeron, Y. & Hély, C. Increases in heat-induced tree mortality could drive reductions of biomass resources in Canada's managed boreal forest. *Landsc. Ecol.* **34**, 403–426 (2019).
- Lloyd, A. H., Rupp, T. S., Fastie, C. L. & Starfield, A. M. Patterns and dynamics of treeline advance on the Seward Peninsula, Alaska. *J. Geophys. Res. Atmos.* **107**, 8161 (2002).
- Wei, Y. et al. The North American carbon program multi-scale synthesis and terrestrial model intercomparison project—part 2: Environmental driver data. *Geosci. Model Dev.* **7**, 2875–2893 (2014).
- Wang, T., Hamann, A., Spittlehouse, D. & Carroll, C. Locally downscaled and spatially customizable climate data for historical and future periods for North America. *PLoS ONE* **11**, e0156720 (2016).
- Rollins, M. G. LANDFIRE: a nationally consistent vegetation, wildland fire, and fuel assessment. *Int. J. Wildland Fire* **18**, 235–249 (2009).
- Rogers, B., Randerson, J. & Bonan, G. High-latitude cooling associated with landscape changes from North American boreal forest fires. *Biogeosciences* **10**, 699–718 (2013).
- Wright, I. J. et al. The worldwide leaf economics spectrum. *Nature* **428**, 821–827 (2004).
- Aerts, R. Nutrient use efficiency in evergreen and deciduous species from heathlands. *Oecologia* **84**, 391–397 (1990).
- Poorter, H., Niinemets, Ü., Poorter, L., Wright, I. J. & Villar, R. Causes and consequences of variation in leaf mass per area (LMA): a meta-analysis. *New Phytol.* **182**, 565–588 (2009).

32. Euskirchen, E., McGuire, A. D., Chapin, F. & Rupp, T. The changing effects of Alaska's boreal forests on the climate system. *Can. J. For. Res.* **40**, 1336–1346 (2010).
33. Nelson, J. L., Zavaleta, E. S. & Chapin, F. S. Boreal fire effects on subsistence resources in Alaska and adjacent Canada. *Ecosystems* **11**, 156–171 (2008).
34. Rupp, T. S., Starfield, A. M., Chapin, F. S. & Duffy, P. Modeling the impact of black spruce on the fire regime of Alaskan boreal forest. *Clim. Change* **55**, 213–233 (2002).
35. Mekonnen, Z. A., Riley, W. J. & Grant, R. F. Accelerated nutrient cycling and increased light competition will lead to 21st century shrub expansion in North American Arctic tundra. *J. Geophys. Res. Biogeosci.* **123**, 1683–1701 (2018).
36. Grant, R. F. Modelling changes in nitrogen cycling to sustain increases in forest productivity under elevated atmospheric CO₂ and contrasting site conditions. *Biogeosciences* **10**, 7703–7721 (2013).
37. Aerts, R. The advantages of being evergreen. *Trends Ecol. Evol.* **10**, 402–407 (1995).
38. Liu, S. et al. The Unified North American Soil Map and its implication on the soil organic carbon stock in North America. *Biogeosciences* **10**, 2915–2930 (2013).
39. Hugelius, G. et al. A new data set for estimating organic carbon storage to 3 m depth in soils of the northern circumpolar permafrost region. *Earth Syst. Sci. Data* **5**, 393–402 (2013).
40. Dentener, F. *Global Maps of Atmospheric Nitrogen Deposition, 1860, 1993, and 2050* (Oak Ridge National Laboratory Distributed Active Archive Center, 2006); <https://doi.org/10.3334/ORNLDAAAC/830>
41. Mekonnen, Z. A., Grant, R. F. & Schwalm, C. Sensitivity of modeled NEP to climate forcing and soil at site and regional scales: Implications for upscaling ecosystem models. *Ecol. Modell.* **320**, 241–257 (2016).
42. Rogers, B. et al. Quantifying fire-wide carbon emissions in interior Alaska using field measurements and Landsat imagery. *J. Geophys. Res. Biogeosci.* **119**, 1608–1629 (2014).
43. Turetsky, M. R. et al. Recent acceleration of biomass burning and carbon losses in Alaskan forests and peatlands. *Nat. Geosci.* **4**, 27–31 (2011).
44. Boby, L. A., Schuur, E. A., Mack, M. C., Verbyla, D. & Johnstone, J. F. Quantifying fire severity, carbon, and nitrogen emissions in Alaska's boreal forest. *Ecol. Appl.* **20**, 1633–1647 (2010).
45. Kasischke, E. S. et al. Alaska's changing fire regime—implications for the vulnerability of its boreal forests. *Can. J. For. Res.* **40**, 1313–1324 (2010).
46. Balshi, M. S. et al. Assessing the response of area burned to changing climate in western boreal North America using a multivariate adaptive regression splines (MARS) approach. *Glob. Change Biol.* **15**, 578–600 (2009).
47. Euskirchen, E., McGuire, A. D., Rupp, T., Chapin, F. & Walsh, J. Projected changes in atmospheric heating due to changes in fire disturbance and the snow season in the western Arctic, 2003–2100. *J. Geophys. Res. Biogeosci.* **114**, G04022 (2009).
48. Bachelet, D., Lenihan, J., Neilson, R., Drapek, R. & Kittel, T. Simulating the response of natural ecosystems and their fire regimes to climatic variability in Alaska. *Can. J. For. Res.* **35**, 2244–2257 (2005).
49. Tape, K., Sturm, M. & Racine, C. The evidence for shrub expansion in northern Alaska and the pan-Arctic. *Glob. Change Biol.* **12**, 686–702 (2006).

Acknowledgements

This research was supported by the Director, Office of Science, Office of Biological and Environmental Research of the US Department of Energy under contract no. DE-AC02-05CH11231 to Lawrence Berkeley National Laboratory as part of the Next-Generation Ecosystem Experiments in the Arctic (NGEE-Arctic) project and the RUBISCO Scientific Focus Area. B.M.R. was funded by NASA's Arctic-Boreal Vulnerability Experiment (ABoVE) and Carbon Cycle Science programmes (NNX17AE13G).

Author contributions

All authors contributed to this work. Z.A.M., W.J.R. and J.T.R. designed the model experiments and implementation of regional fire regime. Z.A.M. performed the simulations and analysed the results. Z.A.M., W.J.R., J.T.R., R.F.G. and B.M.R. contributed extensively to the contents of the manuscript.

Competing interests

The authors declare no competing interests.

Additional information

Supplementary information is available for this paper at <https://doi.org/10.1038/s41477-019-0495-8>.

Reprints and permissions information is available at www.nature.com/reprints.

Correspondence and requests for materials should be addressed to Z.A.M.

Peer review information: *Nature Plants* thanks Emeline Chaste and Winslow Hansen and other, anonymous, reviewers for their contribution to the peer review of this work.

Publisher's note: Springer Nature remains neutral with regard to jurisdictional claims in published maps and institutional affiliations.

© The Author(s), under exclusive licence to Springer Nature Limited 2019